

**Electronic Supplementary information (ESI) for**

**Crystal Growth of Platinum-Ruthenium Bimetallic Nanocrystallite and Their  
Methanol Electrooxidation Activity**

*Tsan-Yao Chen<sup>a,b\*</sup>, Yu-Ting Liu<sup>c</sup>, Hong-Shuo Chen<sup>d</sup>, Kuan-Wen Wang<sup>d</sup>, Cheng-Tao Yang<sup>e</sup>, Tzy-Jiun Mark Luo<sup>b</sup>, Chih-Hao Lee<sup>a,f\*</sup>, and Tsang-Lang Lin<sup>a</sup>*

Affiliations:

<sup>a</sup> Department of Engineering and System Science, National Tsing Hua University,  
Hsinchu 30013, Taiwan

<sup>b</sup> Department of Materials Science and Engineering, North Carolina State University,  
Raleigh, NC 27695, USA

<sup>c</sup> Department of Environmental Science and Engineering, Tunghai University,  
Taichung 40704, Taiwan

<sup>d</sup> Institute of Materials Science and Engineering, National Central University,  
Taoyuan 320, Taiwan

<sup>e</sup> Department of Civil Engineering, National Cheng Kung University, Tainan 701,  
Taiwan

<sup>f</sup> National Synchrotron Radiation Research Center, Hsinchu 30076, Taiwan

\*To whom correspondence should be addressed: Tsan-Yao Chen, email:  
[chencaeser@gmail.com](mailto:chencaeser@gmail.com); Tsang-Lang Lin, email: [tllin@mx.nthu.edu.tw](mailto:tllin@mx.nthu.edu.tw); Tel:  
+886-3-5742671 (O); +886-3-5728445 (Fax)

## 1. XAS data collection, normalization, and model analysis

The heteroatomic intermixes and the unfilled valence orbital states (unfilled d states) of the electrochemical active atoms (Pt) of BiNPs were determined by X-ray absorption spectroscopy (XAS). All the XAS spectra were recorded at the wiggler beam line of BL-17C (for Pt  $L_3$ -edge,  $E_0 = 11564$  eV) and the superconducting wavelength shifter beam line of BL-01C1 (for Ru K-edge,  $E_0 = 22117$  eV) of NSRRC using X-ray grazing incident fluorescence detection by a Lytle detector.<sup>35</sup> Upon data collection, the appropriate filters (Ge and Mo for Pt  $L_3$  and Ru K-edges, respectively) were placed in front of the detector to eliminate the scattering background. The incident and transmitting X-ray through the reference sample was recorded after each XAS scan to obtain the reference spectrum for calibrating the energy of the incident X-ray. For collecting the XAS spectra, the samples were prepared with the identical methods to that of XRD analysis.

The XAS data including the XANES and the EXAFS oscillations ( $\chi(k)$ ), where  $k$  is the photoelectron wave number, were extracted and normalized according to the standard procedures of Athena program (with the code of AUTOBK algorithm 2.93) in the IFEFFIT package (version 1.2.10)<sup>1-4</sup>. Using a Hanning window function forward Fourier transformation (FFT) was performed on the EXAFS region of normalized XAS spectra with the selected  $k$  ranges for the Pt  $L_3$  (from 3.25 to 14.1 Å<sup>-1</sup>)

and Ru *K*-edges (from 2.85 to 13.90 Å<sup>-1</sup>) to generate the radial structure functions (RSF) in the radial space ranging from 0 to 5.0 Å.

To conduct a XAS simulation, the reference structural information of standard Pt, and Ru crystals (obtained from the Inorganic Crystal Structure Database (ICSD) and WebAtoms Database) was implemented in FEFF6.20 program<sup>5</sup> in the IFEFFIT package (version 1.2.10)<sup>1-3</sup> to generate theoretical bond paths of Pt-Pt, Pt-Ru, Ru-Ru, and Ru-Pt. The model of simulating Pt *L*<sub>3</sub>-edge XAS data was based on the cadre of Pt FCC crystal (with a **Fm3m** symmetry), where the number of neighboring atoms in the nearest shell ( $N_{\text{Pt-N}}$ ) is 12 at the interatomic distance ( $R_{\text{Pt-N}}$ ) of 2.772 Å. The bond path of heteroatoms was generated by substituting Pt with Ru in the first coordination shell of the lattice model. For the Ru *K*-edge simulation, the atomic structure model was generated by using the framework of Ru HCP crystal (with a P63/mmc symmetry), where the number of neighboring atoms in the first two nearest shells ( $N_{\text{Ru-N1}}$ ) is 6 at the interatomic distance ( $R_{\text{Pt-N}}$ ) around 2.672 Å.

The obtained RSF function was analyzed using EXAFS simulation (Artemis kits) with appropriate models (the scattering paths of Pt-Pt, Pt-Ru, and Ru-Ru bonding pairs) to investigate the local structural parameters (including the structural parameters of interatomic bond distance ( $R_{ij}$ ), phase shifts ( $\Phi_{ij}$ ), coordination numbers ( $N_j$ ), amplitude reduction factor ( $S_i^2$ ), effective wave backscattering amplitude ( $F_j(k)$ )),

and Debye-Waller factor ( $\sigma_j^2$ ) around X-ray excited atoms in IFEFFIT program with EFEE6.01 code<sup>9-11</sup>. To simplify the EXAFS fitting, the values of  $S_i^2$  of Pt and Ru atoms were fixed at 0.83 which was in good agreement with the theoretical estimation and can be used for different samples with central atoms in a similar chemical state (valence, coordination). Only single scattering paths were considered in fitting the experimental XAS data to prevent unexpected analytical errors (which may be due to the background noises or the multiple scattering effects from the higher order shells). The model simulation of XAS fitting with metal substitution was conducted by incorporating appropriate constrains in a single coordination shell. To evaluate the local structural information around X-ray excited atoms, we adopted independent iterations to avoid the unexpected errors of direct correlation between structural parameters. The  $k^3\chi(k)$  were fitted with all the possible scattering paths for the corresponding FT peaks, where structural parameters of  $\sigma_j^2$ ,  $N_j$ , and the  $R_{ij}$  were treated as adjustable parameters<sup>12</sup>.

## 2. Data collection and model analysis on Small angle X-ray Scattering spectra of core-shell NCs.

The SAXS spectra were collected at the IASW - Small/Wide Angle X-ray Scattering beamline of BL-23A at National Synchrotron Radiation Research Center (NSRRC, Taiwan) by using an incident X-ray wavelength of 0.8857 Å. For collecting the SAXS spectra, the samples were re-dispersed in distilled water in a metal content of 10 mg × ml<sup>-1</sup> and then sealed in a 5 mm thick transmission liquid cell.

All SAXS data were collected at the In-Achromate superconducting wigglers (IASW) beamline at BL-23A of the National Synchrotron Radiation Research Center (NSRRC, Taiwan) with incident X-ray beam at a wavelength of 0.8857 Å (14.0 keV). The SAXS data were corrected for sample transmission, background, and detector sensitivity, and normalized to the absolute scattering scale, namely, scattering cross-section per unit sample volume  $I(Q)$ . Samples (containing ~0.1 mg of NPs and ~1.0 wt% of PVP-40 in distilled water) were sealed in a 3.0 mm thick stainless steel cell using two kapton films (~25 µm thick) as the X-ray windows. With the sample to - detector distance of 1732 mm and 2730 mm, the SAXS data were taken by an area detector covering  $Q$ -range from 0.01 to 0.592 Å<sup>-1</sup>. The obtained scattering functions were analyzed using a to component SAXS model comprising fractal aggregates<sup>1,2</sup> and Hard sphere with Schultz particle size dispersions. By considering a suspension

of spherically symmetric particles with polydispersion of particle size; the scattering intensity can be expressed as the combination of the contributions from the fractal aggregate and the sphere particle with Schultz particle size dispersions as shown in eq

S1:

$$I(Q) = A^F \cdot S(Q)^F \cdot P(Q)^F + A^{HS} \cdot S(Q)^{HS} \cdot P(Q)^{HS} \dots \text{(S1)}$$

where, A is the number density of the aggregates/particles. The structure factor  $S(Q)$  and the particle form factor  $P(Q)$  both depend on the momentum transfer  $Q$ . Symbols of  $F$  (fractal aggregate) and  $HS$  (hard sphere with Schultz distribution) on the superscript identify which model the parameter belongs to.  $P(Q)^F$  is the scattering from randomly distributed spherical "building block" particles, having radius  $R_0$ , volume fraction  $\phi$ , and scattering length density difference  $\Delta\rho = \rho_1 - \rho_2$ .

$$P(Q) = \phi V_p \Delta\rho^2 F(QR_0)^2 \dots \text{(S1a)}$$

where  $V(p) = \frac{4}{3}\pi R_0^3$  and

$$F(QR_0) = \frac{3[\sin(QR_0) - QR_0 \cos(QR_0)]}{(QR_0)^3} \dots \text{(S1b)}$$

The structure factor  $S(Q)^F$  is calculated as:

$$S(Q) = 1 + \frac{\sin[(D_f - 1)\tan^{-1}(q\xi)]}{(QR_0)^{D_f}} \frac{D_f \Gamma(D_f - 1)}{[1 + 1/(Q^2 \xi^2)]^{(D_f - 1)/2}} \dots \text{(S1c)}$$

where  $\xi$  corresponds to the overall coherent length (size) of aggregates,  $D_f$  is the self-similarity packing dimension of nanoparticles in aggregates, and  $R_0$  is the radius of randomly distributed spherical "building block" particles in the aggregate.  $\Gamma(D_f - 1)$

is a gamma function.

The returned value is scaled to units of [cm<sup>-1</sup> sr<sup>-1</sup>], in absolute scale. The (normalized) Schulz distribution is:

$$f(R) = (z+1)^{z+1} x^z \frac{\exp[-(z+1)x]}{R_{avg} \Gamma(z+1)} \dots (S1d)$$

where R<sub>avg</sub> is the mean radius specified by W and x = R/R<sub>avg</sub>, z is related to the polydispersity,  $p = \sigma/R_{avg}$ , by  $z = 1/p^2 - 1$ . σ<sup>2</sup> is the variance of the distribution.

The distribution can be plotted for the radius and polydispersity in the coef\_sch wave using the macro "PlotSchulz\_Distribution()". In this macro the N<sup>th</sup> moment of size distribution is equal to:

$$\langle R^N \rangle = \frac{R_{avg}^N}{(z+1)^N} \frac{(z+N)!}{z!} \dots (S1e)$$

The form factor is normalized by the average volume, using the 3<sup>rd</sup> moment of R:

$$\langle V \rangle = \frac{4\pi}{3} \langle R_{avg} \rangle^3 \frac{(z+3)(z+2)}{(z+1)^2} \dots (S1f)$$

If the scale factor W[0] is set equal to the particle volume fraction, φ, the returned value is the differential macroscopic scattering cross-section (scattered cross-section per unit sample volume per unit solid angle).

$$I(q) = \left(\frac{4\pi}{3}\right)^2 N_0 \Delta\rho^2 \int_0^\infty f(R) R^6 F^2(QR) dR \dots (S1g)$$

where N<sub>0</sub> is the total number of particles per unit volume, and Δρ = w[3]-w[4], is the difference in scattering length density. The number of particles per unit volume having size between R and R + dR is equal to  $N(R)dR = N_0 f(R)dR$ . The Macro

PlotSchulz Distribution plots the function  $f(R)$  vs R.

The scattering amplitude for a sphere is given by eq S1b. However, no interparticle interference effects are included in this calculation. Interparticle interference  $S(Q)$  should be included by:

$$I(Q) = N_0 S(Q) P(Q) \dots (\text{S1h})$$

where  $P(Q)$  is the form factor. Some other relations of interest are:

$$N_0 = \frac{\phi}{\langle V \rangle}$$

Guinier radius:

$$R_g = \sqrt{\frac{3(R^3)}{5(R^6)}} = R_{avg} \sqrt{\frac{3(z+8)(z+7)}{5(z+1)^2}} \dots (\text{S1i})$$

Total interfacial surface area per unit sample volume:

$$S_V = 4\pi \langle R^2 \rangle N_0 = \frac{3\phi}{R_{avg}} \frac{(z+1)}{(z+3)} \dots (\text{S1j})$$

Accordingly, the forward scattering cross-section:

$$I(Q=0) = N_0 \langle V^2 \rangle \Delta \rho^2 R_{avg}^3 \frac{(z+6)(z+5)(z+4)}{(z+1)^3} \dots (\text{S1k})$$

These values are calculated using the macro "NumberDensity\_Schulz()" and use the current values in the coef\_sch wave.  $W[0]$  (volume fraction or arbitrary scale) and  $(W[3] - W[4])^2$  (contrast) are multiplicative factors in the model and are perfectly correlated. Only one of these three parameters should be left free during model fitting.  $W[2]$  (polydispersity ( $p$ )) must be between  $0 < p < 1$ .

Reference: Guinier, A. and G. Fournet, "Small-Angle Scattering of X-Rays", John

Wiley and Sons, New York, (1955). G. V. Schulz, Z. Phys. Chem., 43 (1935) 25. M.

Kotlarchyk and S-H. Chen, J. Chem. Phys. 79 (1983) 2461-2469, eqn 25-29.

As shown in Figure S1, all experimental data is well fitted by the proposed model. The least-square fitting curve is denoted by solid line; where the fitting curve of the fractal model is denoted by a dashed line and the hard sphere particle model with Shultz distribution of particle size is shown by dash-dotted line.

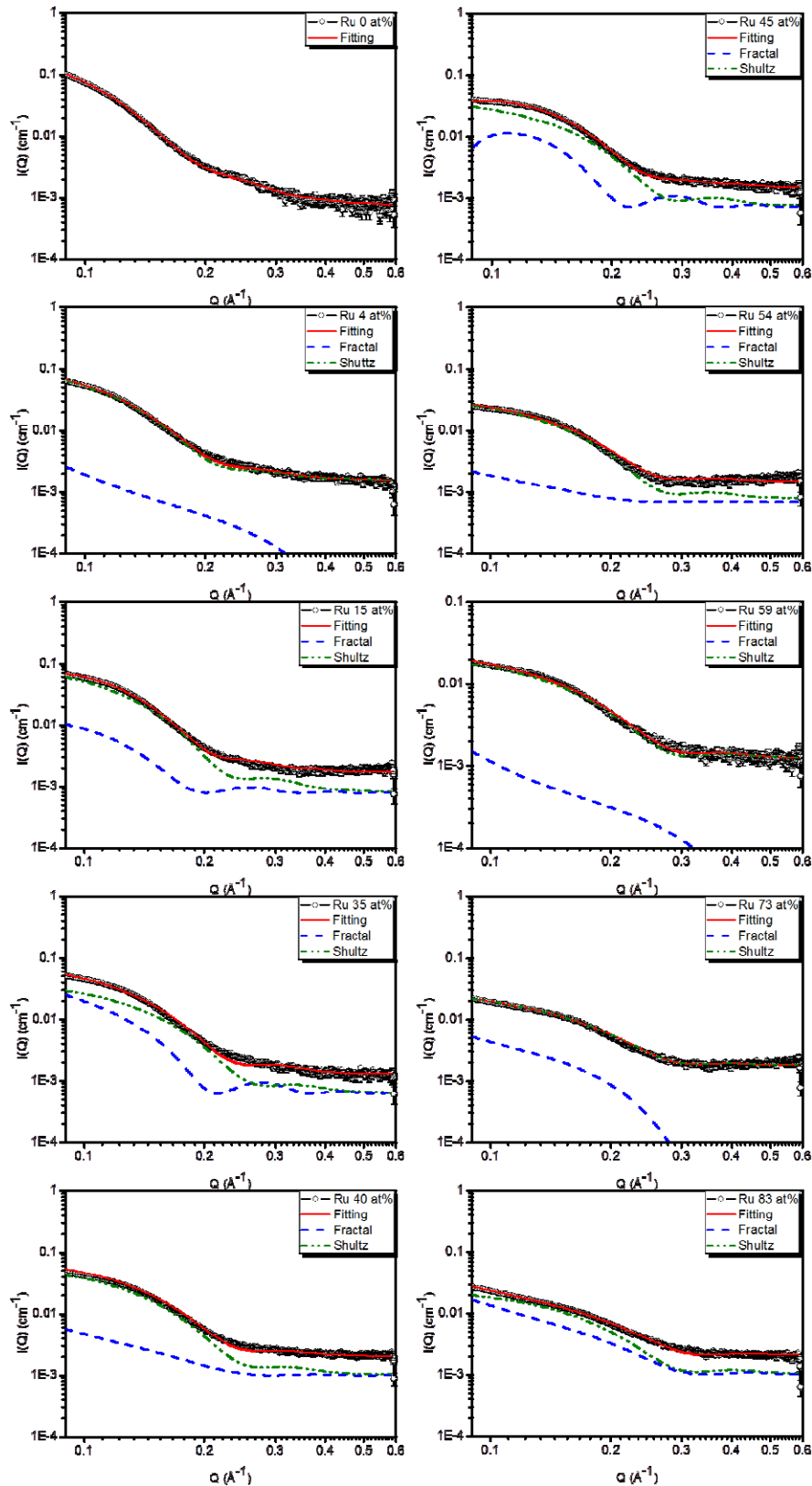


Figure S1. The SAXS patterns of BiNPs with fitting curves.

## 2. X-ray diffraction data collection and analysis on lattice strain estimation

The crystal structure evolutions of BiNPs with respecting to the Pt/Ru ratios were elucidated by using X-ray diffraction (XRD). The XRD patterns were collected at the superconducting wavelength shifter beamline of BL-01C2 of NSRRC and at the bending-magnet beamline of BL-12B2 of SPring-8 (Japan) by the two dimensional area detectors of IP-MAR3450 and CCD-Quantum210, respectively. During data collection, the incident X-ray wavelength and exposure time were set to be 1.3332 Å and 2 min, respectively. For XRD measurements, the samples were prepared by spin coating 150 µl of the re-dispersed BiNPs on a 1.5 × 3.0 cm<sup>2</sup> Si (111) wafer and dried at 120°C for 2 h.

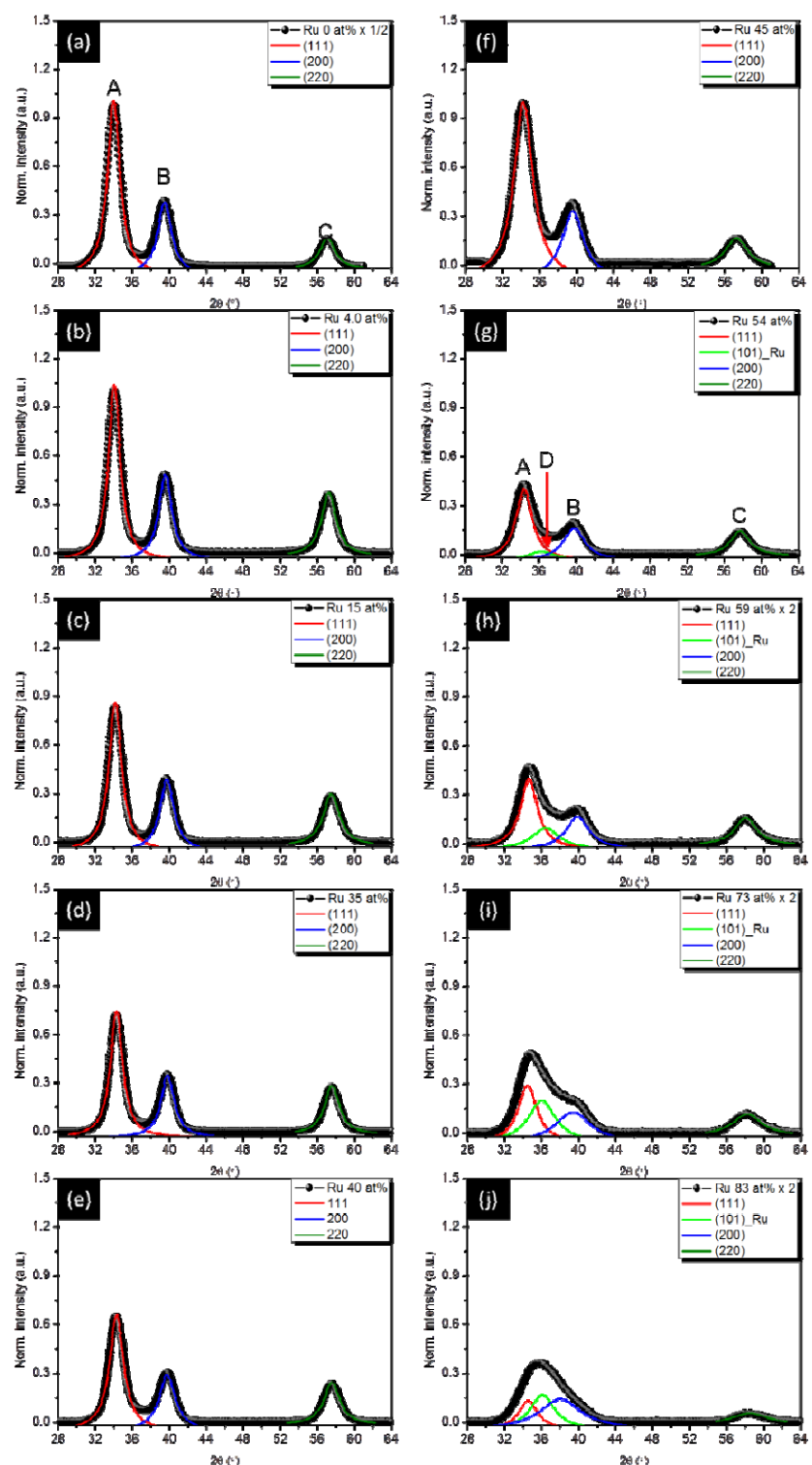


Figure S2. The XRD patterns with the fitting curves (obtained by peak de-convolution using multiple peak Lorentz function)

Table S1. X-ray diffraction determined structure parameters of BiNPs with different Ru contents.

Ru at%	lattice constant $a(hkl)$ ( $\text{\AA}$ ) $\pm 0.005 \text{ \AA}$		
	$a(111)$	$a(200)$	$a(220)$
0	3.925	3.923	3.923
4	3.918	3.916	3.914
15	3.907	3.904	3.896
35	3.892	3.893	3.893
40	3.891	3.887	3.893
45	3.888	3.885	3.890
54	3.884	3.879	3.883
59	3.874	3.874	3.861
73	3.868	3.864	3.852
83	3.865	3.855	3.833

### 3. Data analysis on X-ray Absorption Spectroscopy

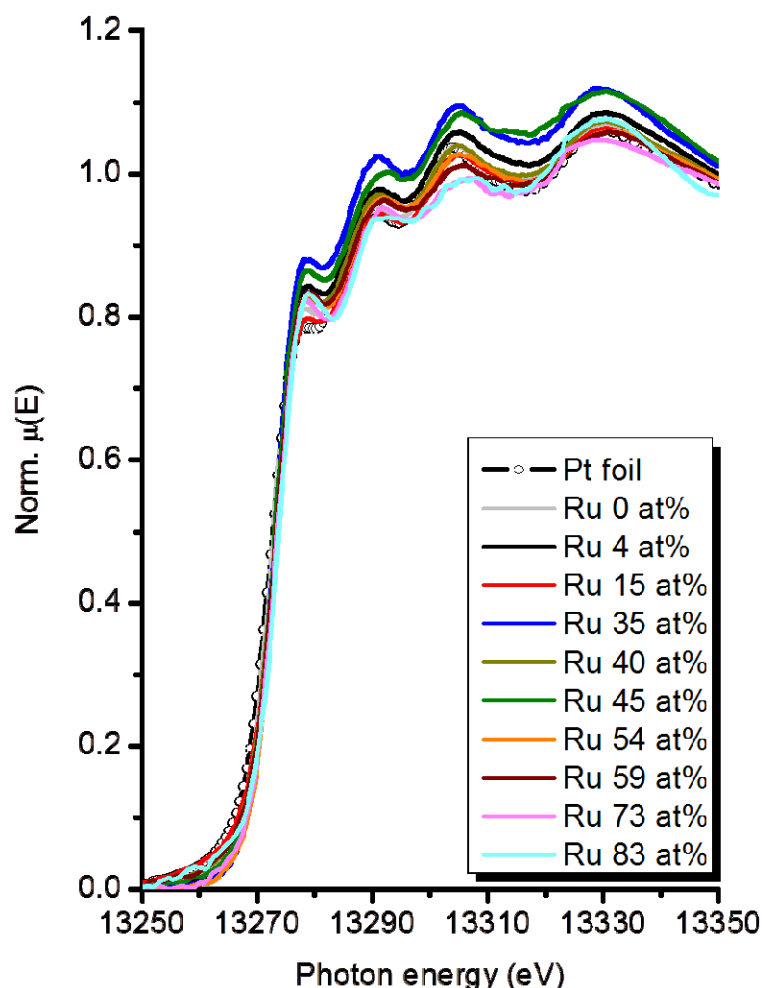


Figure S3. Pt  $L_2$ -edge XANES spectra of Pt foil compared with that of BiNPs with different Ru contents.

The highest weight line intensity and weakest post-edge oscillation are clear indications for the presence of strong charge transition probability ( $2p_{3/2} - 5d_{3/2}$ ) and the low z elements around Pt atoms of Ru 83 at% catalysts among all BiNPs.

Table S2. Pt L<sub>3</sub>-edge XANES linear combination analysis derived chemical composition distributions of BiNPs.

Ru at %	Pt 0 (mole%)	H <sub>2</sub> PtCl <sub>6</sub> (mole%)
0	87.6	12.4
4	83.7	16.3
15	89.2	10.8
35	83.5	16.5
40	82.2	17.8
45	79.1	20.9
54	83.3	16.7
59	83.2	16.8
73	84.6	15.4
83	78.0	22.0

#### 4. Electrochemical performance of BiNPs

The CV curves for measuring the MOR of electrocatalysts was conducted by a CHI-600 potentiostat equipped with a homemade three electrodes electrochemical system (comprising a working electrode of NPs coated FTO glass, a counter electrode of 10 × 10 mm<sup>2</sup> platinum foil, and a standard SCE reference electrode). The electrolyte is an aqueous solution of 0.5 M methanol and 0.5 M H<sub>2</sub>SO<sub>4</sub>.

##### 4.1 Estimation on surface to bulk ratio of nanoparticles

From a geometric standpoint, the surface to bulk ratio ( $\rho_{S-V}$ ) for a particle can be estimated by using the following equation:

$$\rho_{S-V} = \frac{n_s}{n_t} \dots (S2)$$

where  $n_s$  and  $n_t$  denote the number of surface atoms and total number of atoms, respectively. The  $n_s$  can be determined by dividing the occupied area ( $P_s \times S'$ ,  $P_s$  denotes the surface atomic packing factor of a surface, and the surface area of the particle  $S'$  is equal to  $4\alpha\pi R^2$  with radius  $R$ ) by the cross section area of particle ( $\pi r^2$ , where  $r$  denotes the radius of the atom). For a particle,  $S'$  can be determined by multiplying the surface area of the spherical particle by a shape modification factor ( $\alpha$ ) that considers the extent of interfacet truncation. Therefore we can determine  $n_s$  by using Eq. S3.

$$n_s = P_s \frac{S'}{\pi r^2} = P_s \frac{4\alpha\pi R^2}{\pi r^2} = 4\alpha P_s \frac{R^2}{r^2} \dots (S3)$$

The volume of a particle occupied by atoms ( $V_L$ ) can be calculated by combining the half volume of the surface atoms ( $0.5 \times n_s \times V_a$ ) and the volume of the interior atoms ( $n_i \times V_a$ ), where  $V_a$  denotes the atom volume. If a particle has a volume of  $V_P$ , the occupied volume can be presented as follows by adopting a bulk lattice atomic packing factor,  $P_L$  (Eq. S4).

$$V_L = P_L \times V_P \dots (S4)$$

By combining Eq. (S3) and Eq. (S4), we can obtain the following relationship:

$$V_L = n_i V_a + \frac{1}{2} n_s V_a = P_L V_P \Rightarrow n_i + \frac{1}{2} n_s = P_L \frac{V_P}{V_a} = P_L \frac{R^3}{r^3} \dots (S5)$$

Here, the total number of atoms in a particle can be represented as  $n_t = n_i + n_s$ .

According to Eq. (S3) and Eq. (S5),  $n_t$  can be represented as:

$$n_t = P_L \frac{R^3}{r^3} + 2\alpha P_S \frac{R^2}{r^2} \dots \text{(S6)}$$

therefore,  $\rho_{S-V}$  is obtained from the following numerical representation:

$$\frac{n_s}{n_t} = \frac{4\alpha P_S \frac{R^2}{r^2}}{P_L \frac{R^3}{r^3} + 2\alpha P_S \frac{R^2}{r^2}} = \frac{4\alpha P_S}{P_L \frac{R}{r} + 2\alpha P_S} \dots \text{(S7)}$$

Because the shape factor parameters and the packing factors are dominated by particle shape,  $\rho_{S-V}$  is inversely proportional to the radius of the particle (R). This relationship is represented in Figure S4.

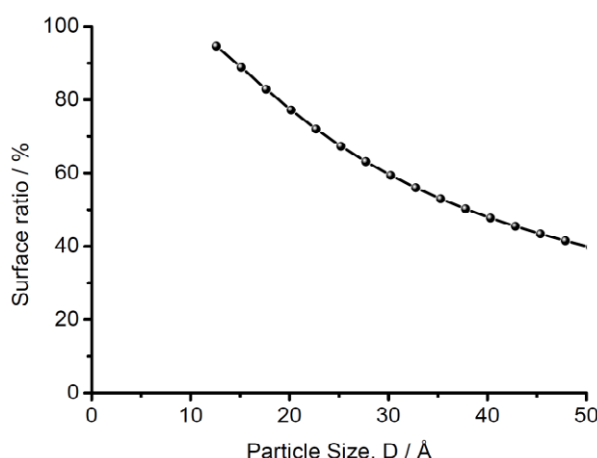


Figure S4. The surface to bulk ratio of sphere nanoparticles as a function of particle size. For spherical particles  $\alpha = 1$ , and for ellipsoid particles  $1 < \alpha < 2$ .

#### 4.2. Estimation of the theoretical surface area (TSA) of BiNPs

To simplify the estimation, the NPs are drawn as a hard sphere particle corresponding to a surface area ( $A_{NPs}$ ) of  $4\pi R_{NPs}^2$ . The parameters of  $R_{NPs}$  denote the radius of the particle. Meanwhile, the weight of each particle is represented as  $M_{NPs} = V_{NPs} \times \rho_{NPs}$ . The parameters of  $\rho_{NPs}$  and  $V_{NPs}$  denote the mass density and volume of individual particle. Consequently, the theoretical specific surface area (TSA) per gram of NPs could be estimated by adopting the density of Pt and Ru into following equation:

$$TSA = \frac{1}{M_{NPs}} \times A_{NPs} = \frac{A_{NPs}}{V_{NPs} \times \rho_{NPs}} \dots (S8)$$

where the volume of the particle is represented as  $V_{NPs} = \frac{4}{3}\pi R^3$  and the mass density can be estimated by considering the weighting of two components in the NPs.

Table S3. The surface to bulk ratio (ns/nt) and theoretical surface area (TSA) of BiNPs derived from theoretical surface area estimation. The rest of structure parameters were determined by SAXS model analysis.

Ru at%	R <sub>avg</sub> (Å)	TSA (m <sup>2</sup> g <sup>-1</sup> )	ns/nt (%)	D <sub>avg</sub> (Å)	P (D <sub>avg</sub> %)
0	20.6	123.5	38.9	41.2	28.7
4	18.6	145.5	42.2	37.2	18.4
16	17.8	165.5	43.7	35.6	14.2
35	17.4	184.1	44.5	34.8	13.1
40	16.4	200.1	46.6	32.8	13.7
45	15.4	210.3	47.0	30.8	10.4
54	15.2	224.1	49.3	30.4	11.3
59	13.8	265.2	53.0	27.6	9.5
73	13.4	294.1	54.2	26.8	12.9
83	12.6	316.7	56.6	25.2	9.4

## Reference

1. Lin, J.-M.; Lin, T.-L.; Jeng, U.-S.; Zhong, Y.-J.; Yeh, C.-T.; Chen, T.-Y., Fractal aggregates of the Pt nanoparticles synthesized by the polyol process and poly(N-vinyl-2-pyrrolidone) reduction. *Journal of Applied Crystallography* **2007**, *40*, s540-s543.
2. Teixeira, J., Small-angle scattering by fractal systems. *Journal of Applied Crystallography* **1988**, *21*, 781-785.
3. Bartlett, P.; Ottewill, R. H., A neutron scattering study of the structure of a bimodal colloidal crystal. *Journal of Chemical Physics* **1992**, *96*, 3306.
4. Wu, R.-J.; Wu, J.-G.; Tsai, T.-K.; Yeh, C.-T., Use of cobalt oxide CoOOH in a carbon monoxide sensor operating at low temperatures. *Sensors and Actuators B* **2006**, *120* 104-109.
5. Cohen, J. L.; Volpe, D. J.; Abruna, H. D., Electrochemical determination of activation energies for methanol oxidation on polycrystalline platinum in acidic and alkaline electrolytes. *Physical Chemistry Chemical Physics* **2007**, *9*, 49-77.